# Shock wave structure in a strongly nonlinear lattice with viscous dissipation

E. B. Herbold[1] and V. F. Nesterenko[1,2]
[1]*Department of Mechanical and Aerospace Engineering, University of California at San Diego, La Jolla, California 92093-0411, USA*
[2]*Materials Science and Engineering Program, University of California at San Diego, La Jolla, California 92093-0418, USA*
(Received 27 June 2006; published 26 February 2007)

The shock wave structure in a one-dimensional lattice (e.g., granular chain of elastic particles) with a power law dependence of force on displacement between particles ($F \propto \delta^n$) with viscous dissipation is considered and compared to the corresponding long wave approximation. A dissipative term depending on the relative velocity between neighboring particles is included to investigate its influence on the shape of a steady shock. The critical viscosity coefficient $p_c$, defining the transition from an oscillatory to a monotonic shock profile in strongly nonlinear systems, is obtained from the long-wave approximation for arbitrary values of the exponent $n$. The expression for the critical viscosity is comparable to the value obtained in the numerical analysis of a discrete system with a Hertzian contact interaction ($n=3/2$). The expression for $p_c$ in the weakly nonlinear case converges to the known equation for the critical viscosity. An initial disturbance in a discrete system approaches a stationary shock profile after traveling a short distance that is comparable to the width of the leading pulse of a stationary shock front. The shock front width is minimized when the viscosity is equal to its critical value.

DOI: 10.1103/PhysRevE.75.021304 PACS number(s): 45.70.−n, 05.45.Yv, 46.40.Cd, 43.25.+y

## I. INTRODUCTION

It is well known that one-dimensional and ordered two- and three-dimensional lattices of particles support compressive strongly nonlinear solitary waves for "normal" nonlinear interaction laws between particles [1]. For example, these waves exist when the force between particles exhibits a power-law dependence on displacement ($F \propto \delta^n$) for $n>1$ [2–5]. The long wave approximations for power-law interactions have exact solutions for compressive solitary waves in nondissipative particle lattices. When lattices are statically compressed they exhibit a dynamic nonlinear behavior that can be tuned [6] from the strongly to the weakly nonlinear regime. However, dissipation significantly attenuates compression pulses in many experimental settings [1,6,7] in the strongly and weakly nonlinear regimes and should be included to model real systems.

There have been a number of analytical and numerical studies that introduce dissipation into the equations of motion for discrete systems. The behavior of a viscous granular gas was investigated [8] using a viscous drag term depending on the velocity of individual particles. Coefficients of restitution were used to investigate inelastic collisions between two particles [9,10] and viscoelastic interactions were introduced in [11,12]. Attenuation in a one-dimensional lattice is analyzed in [13,14]. In [15] coupled dashpots representing viscous dissipation depending on the relative motion between atoms were introduced for the investigation of steady shock waves in anharmonic spring-mass systems. The influence of Stokes drag force, which is a function of particle velocity, and damping depending on the relative motion of particles on enveloped solitons in anharmonic discrete lattices was considered in [16].

Recent experimental and numerical work on pulse propagation in lattices immersed in media with different viscosities (air, oil, and glycerol) [17] demonstrated that a dissipative term based on the relative velocities between particles affect the wave propagation more significantly than Stokes drag. The mechanism of this phenomenon is related to fluid being expelled from and returning to the contact area during dynamic particle interaction corresponding to an increase and decrease of contact force.

The dissipation process influences the behavior of media in the transition area within the shock front and determines the shape of shock profile. For example, in a weakly nonlinear system described by the Korteweg de Vries (KdV) equation, two qualitatively different shock profiles exist depending on the value of the viscosity [18]; oscillatory if below the critical value and monotonic if above. These two profiles also appear experimentally in strongly nonlinear systems using geometrically identical lattices of lead and steel particles under similar loading conditions [1]. The energy dissipation in the strongly nonlinear lead particle lattice is attributed to the significant plastic deformation in the vicinity of the particle contact, which resulted in a monotonic shock profile.

To the best of our knowledge, there is no result for the critical viscosity that ensures a transition from an oscillatory to a monotonic shock profile in strongly nonlinear discrete lattices (e.g., one-dimensional granular chains) or in the corresponding long-wave approximations.

This paper studies the effects of a dissipative term on the type of shock wave profiles (i.e., monotonic or oscillatory) in a discrete strongly nonlinear system using numerical analysis. A dissipative term based on the relative velocity between neighboring particles is introduced in the discrete equations and a critical viscosity is found using the long wave approximation. The numerical results are compared to the analytical treatment of the same system in the context of the long-wave approximation.

## II. EQUATIONS OF MOTION FOR A STRONGLY NONLINEAR DISSIPATIVE DISCRETE LATTICE

In the general case the interaction law in a nondissipative one dimensional lattice can be described by a function of the

 

relative displacements $f(u_i-u_{i+1})$ between neighboring particles, where $u_i$ is the displacement of the $i$th particle. To account for viscous dissipation, a term based on the relative velocities between particles [15–17] is included in the description

$$m\ddot{u}_i = f(u_{i-1}-u_i) - f(u_i-u_{i+1}) + \mu(\dot{u}_{i-1} - 2\dot{u}_i + \dot{u}_{i+1}), \quad (1)$$

where $m$ is the mass and $\mu$ is the viscosity coefficient. A compressive solitary wave exists for Eq. (1) in the absence of dissipation and a stationary shock wave exists when dissipation is included for a "normal" interaction law in the continuum approximation of this discrete system [1,19]. The term "normal" refers to an increasing repulsive potential as the distance between particle centers decreases ($f''>0$) [1]. In the case of "abnormal" interactions ($f''<0$) solitary and shock rarefaction waves may exist in the frame of the long wave approximation. The various properties of these two types of waves are discussed in [1]. The existence of solitary waves in a nondissipative discrete lattice for "normal" interactions is proven in [19].

As a subset of Eq. (1), particles interacting according to a power-law potential represent a relatively broad class of interactions where exact solutions of long-wave approximations can be found for solitary waves [1–5,20]. Numerical analyses for various values of $n$ agree well with the results obtained in the long-wave approximation [14,21,22]. The system of equations using a power law potential including a viscous dissipation term is

$$\ddot{u}_i = A_n(u_{i-1}-u_i)^n - A_n(u_i-u_{i+1})^n + p(\dot{u}_{i-1} - 2\dot{u}_i + \dot{u}_{i+1}), \quad (2)$$

where $A_n$ depends on the geometry of the region of contact and the material properties. The damping coefficient $p$ is defined $p=\mu/m$, where $\mu$ is analogous to the constant used for a dashpot model [15,16]. The classical Hertzian interaction between perfectly elastic spherical particles is a special case of Eq. (2) when $n=3/2$. In this case, experimental results agree qualitatively with the long-wave approximation and numerical calculations for a one dimensional discrete particle lattice made from various types of materials [1,6,7,27,28]: though dissipation was noticeable in all of the experiments.

## III. THE LONG WAVE APPROXIMATION AND CRITICAL VISCOSITY

The long wave approximation can be derived from the strongly nonlinear Eq. (2) by assuming that the particle diameter, $a=2R$, is significantly smaller than the propagating wavelength $L$ so that $\epsilon \equiv a/L \ll 1$, similar to [1,23],

$$u_{tt} = -c_n^2\left[(-u_x)^n + \frac{na^2}{24}((n-1)(-u_x)^{n-2}u_{xx}^2 - 2(-u_x)^{n-1}u_{xxx})\right]_x + pa^2u_{txx}, \quad (3)$$

where $c_n^2=A_na^{n+1}$. Terms of higher order are omitted in the expansions of Eq. (2) as well as the convective derivative, which is valid for a certain range of wave amplitudes [1]. It should be noted that the expression for the long-wave sound speed $c_0$ can be obtained based on the linearization of Eq. (3), $c_0=c_n\sqrt{n}\xi_0^{(n-1)/2}$ [1], where $\xi_0$ is the initial strain due to static compression. In the case of linear media, $n=1$, Eq. (3) is reduced to the well known Boussinesque equation with a linear dispersive and dissipation term. Stationary solutions of Eq. (3) without the viscous term have been discussed in [1] and verified numerically in [14,21,22,24–26] for various values of $n$.

We would like to analyze the stationary shock solutions of Eq. (3) $u(x,t)=u(x-V_{sh}t)$, where $V_{sh}$ is the shock wave speed. This solution satisfies the following, Eq. (4), where the strain is defined as $\xi(x)\equiv -u_x$

$$\frac{V_{sh}^2}{c_n^2}\xi_x = \left[\xi^n + \frac{na^2}{24}((n-1)\xi^{n-2}\xi_x^2 + 2\xi^{n-1}\xi_{xx})\right]_x - \frac{pa^2V_{sh}}{c_n^2}\xi_{xx}. \quad (4)$$

The variable replacement $z=\xi^{(n+1)/2}$ is used to simplify Eq. (4), which can be integrated from $x$ to $\infty$ with the boundary conditions $z(+\infty)=z_0$, and $z_x(x=+\infty)=z_{xx}(x=+\infty)=0$,

$$\frac{V_{sh}^2}{c_n^2}z^{2/(n+1)} = z^{2n/(n+1)} + \frac{a^2n}{6(n+1)}z^{(n-1)/(n+1)}z_{xx} - \frac{2pa^2V_{sh}}{c_n^2(n+1)}\frac{z_x}{z^{(n-1)/(n+1)}} + C_1. \quad (5)$$

Equation (5) is simplified further using the variable replacements $z=(V_{sh}/c_n)^{(n+1)/(n-1)}y$ and $x=a\eta\sqrt{n/6(n+1)}$,

$$y_{\eta\eta} - \bar{p}y^{-2(n-1)/(n+1)}y_\eta + y - y^{-(n-3)/(n+1)} + y^{-(n-1)/(n+1)}C_2 = 0, \quad (6)$$

where $\bar{p}$ represents the dimensionless viscosity:

$$\bar{p} \equiv \frac{2ap}{V_{sh}}\sqrt{\frac{6}{n(n+1)}}. \quad (7)$$

Equation (6) can be expressed as an equation for the nonlinear oscillator moving in a "potential field" $W(y)$ with a nonlinear "dissipative" term,

$$y_{\eta\eta} = -\frac{\partial W(y)}{\partial y} + \bar{p}y^{-2(n-1)/(n+1)}y_\eta, \quad (8)$$

where the "potential" $W(y)$ is defined

$$W(y) = \frac{1}{2}y^2 - \frac{n+1}{4}y^{4/(n+1)} + C_3y^{2/(n+1)}. \quad (9)$$

The relations between constants $C_3$, $C_2$, and $C_1$ are

$$C_3 = \frac{n+1}{2}C_2 = \frac{n+1}{2}\left(\frac{c_n}{V_{sh}}\right)^{2n/(n-1)}C_1. \quad (10)$$

As a representative example of a real system where particles interact according to Hertz law, the potential $W(y)$ is plotted in Fig. 1 and five curves are shown for different values of $C_3$ using $n=3/2$. Each of the curves (1)–(4) in Fig. 1 has a local minimum at $y_2$ (indicated by arrows) and a local

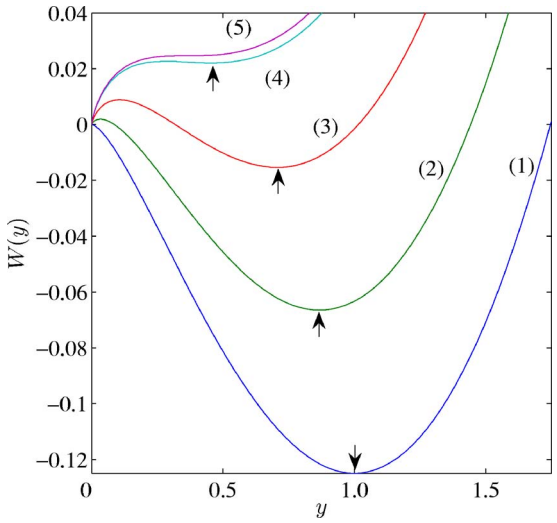


FIG. 1. (Color online) Plot of the potential $W(y)$ for the strongly nonlinear wave equation using $n=3/2$ (Hertzian potential). Curve (1): $C_3=0$; curve (2): $C_3=5/81$; curve (3): $C_3=10/81$; curve (4): $C_3=0.18$; curve (5): $C_3=5/27$ (limiting case where there is no local extrema). The local maximum of each curve corresponds to the position of $y_1$, which is the initial state in front of the shock wave. The arrows indicate the minimum of $W(y)$, $y_2$, which is the final state in the shock wave.

maximum at $y_1$. Stationary solitary waves are not permitted in the system represented by curve (5) where there are no local extrema (i.e., there is no potential well).

The motion of a nondissipative oscillator with a total energy equal to the local maximum of $W(y)$ at $y_1$ corresponds to the solitary wave solution [1]. Nondissipative oscillations corresponding to curve (4) have an initial energy close to the local maximum of $W(y)$, which results in a relatively small range of "displacement" $y$. This type of behavior is related to weakly nonlinear waves, in which an initial strain is high with respect to the dynamic change in strain caused by the passing wave. Curve (1) corresponds to the strongly nonlinear case of a sonic vacuum where the initial strain is equal to zero and the ratio of the strain in the wave to the initial strain is infinite.

The effective potential energy $W(y)$ has local extrema if $C_3$ is positive and smaller than some critical value (5/27 in case if $n=3/2$) for $n>1$ [1]. The local minimum and maximum values of the potential in the presence of dissipation can be interpreted as the initial and final states for the stationary shock wave. The local maximum of $W(y)$ at $y_1$ is related to the initial strain in front of the shock wave and the local minimum at $y_2$ corresponds to the final equilibrium state. Each pair of $y_1$ and $y_2$ are uniquely defined by the values of $n$ and $C_3$.

It is possible to express $C_3$ in terms of $V_{\mathrm{sh}}$ and $\xi_0$ for a solitary or shock wave solutions using the condition at the local maximum at $y_1$, $\partial W(y)/\partial y|_{y=y_1}=0$,

$$C_3 = \frac{n+1}{2}\left(\frac{c_n}{V_{\mathrm{sh}}}\right)^{2/(n-1)} \xi_0 \left[1 - \left(\frac{c_n}{V_{\mathrm{sh}}}\right)^2 \xi_0^{n-1}\right]. \tag{11}$$

Weakly and strongly nonlinear regimes can be determined by the values of $V_{\mathrm{sh}}$ with respect to sound speed $c_0$, which also determines $C_3$. For example, when $V_{\mathrm{sh}}$ approaches $c_0$ then $C_3$ approaches 5/27 when $n=3/2$.

The behavior of the strain in a stationary shock profile in the vicinity of the final state of the shock wave can be analyzed by linearizing Eq. (6) representing $y$ as sum of two terms,

$$y(\eta) = y_2 + \Psi(\eta), \tag{12}$$

where $\Psi(\eta) \ll y_2$. It is assumed that the transition from an oscillatory to a monotonic shock profile can be identified by the behavior of solutions in the vicinity of the final state represented by $y_2$. Substituting Eq. (12) into Eq. (6) results in the linear equation,

$$\Psi_{\eta\eta} - \bar{p} y_2^{-2(n-1)/(n+1)} \Psi_\eta + \frac{2}{n+1}(n - y_2^{-2(n-1)/(n+1)})\Psi = 0. \tag{13}$$

In the derivation of Eq. (13) $C_3$ was expressed as a function of $y_2$ based on equation for the derivative of the potential function being equal zero at $y=y_2$ $\partial W(y)/\partial y|_{y=y_2}=0$,

$$C_3 = \frac{n+1}{2}[y_2^{2/(n+1)} - y_2^{2n/(n+1)}]. \tag{14}$$

Equation (13) is an equation for a linear oscillator with dissipation. It has the solution

$$\Psi(\eta) = b_1 \exp\left[\left(\frac{\bar{p}}{2} y_2^{-2(n-1)/(n+1)} \pm g(y_2)\right)\eta\right], \tag{15}$$

where $b_1$ is a constant and

$$g(y_2) = \frac{1}{2}\left[\bar{p}^2 y_2^{-4(n-1)/(n+1)} - \frac{8}{n+1}(n - y_2^{-2(n-1)/(n+1)})\right]^{1/2}. \tag{16}$$

Imaginary values of $g(y_2)$ correspond to an oscillatory profile and the transition from an oscillatory to a monotonic shock profile occurs when $g(y_2)=0$. Thus the critical damping coefficient can be derived based on Eq. (16). It depends on the properties of the potential function, including the power law exponent $n$, and position of the local minimum $y_2$:

$$\bar{p}_c = \sqrt{\frac{8}{n+1}(n y_2^{4(n-1)/(n+1)} - y_2^{2(n-1)/(n+1)})}. \tag{17}$$

In the case of a sonic vacuum, the local minimum is at $y_2 = 1$ [curve (1) in Fig. 1], which corresponds to $C_2=0$ in Eq. (6). Using $y_2=1$ in Eq. (17) gives the expression for the dimensionless critical viscosity corresponding to the transition from an oscillatory to a monotonic shock profile in a sonic vacuum for arbitrary $n$,

$$\bar{p}_{c,\mathrm{sv}} = \sqrt{8(n-1)/(n+1)}. \tag{18}$$

Combining Eq. (18) with Eq. (7) results in a dimensional form of the critical viscosity:

$$p_{c,\mathrm{sv}} = V_{\mathrm{sh}}/a\sqrt{n(n-1)/3}. \tag{19}$$

This critical viscosity depends on the amplitude of the shock wave through its speed $V_{\mathrm{sh}}$, which is related to the final par-

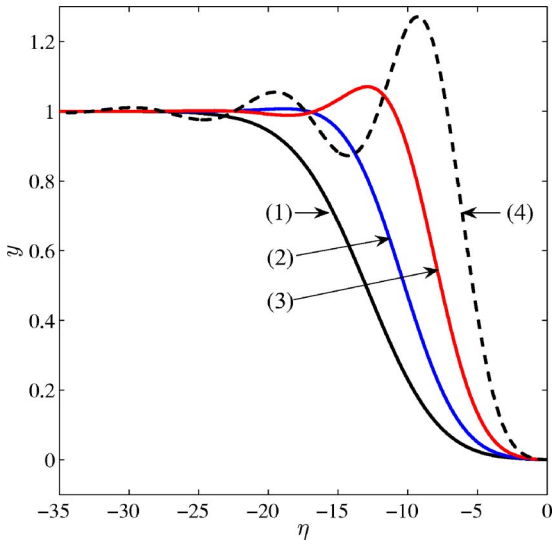


FIG. 2. (Color online) Oscillatory and monotonic shock waves in a "sonic vacuum" ($C_3=0$). Each curve is a plot of the numerical solution of Eq. (6) for $n=3/2$ (Hertzian potential) and the corresponding $\bar{p}_{c,\mathrm{sv}}=1.265$. The curves (1)–(4) in the figure show the solution at different values of $\bar{p}$. Curve (1): $\bar{p}=\bar{p}_{c,\mathrm{sv}}$; curve (2): $\bar{p}=0.75\bar{p}_{c,\mathrm{sv}}$; curve (3): $\bar{p}=0.5\bar{p}_{c,\mathrm{sv}}$; curve (4): $\bar{p}=0.25\bar{p}_{c,\mathrm{sv}}$.

ticle velocity or the strain behind the shock. The critical viscosity can be close to zero for very small amplitudes of the shock in a sonic vacuum since $V_{\mathrm{sh}}$ is not restricted by the sound speed.

It is interesting to investigate the validity of Eq. (18), derived using Eq. (13) in the vicinity of $y_2$, in the entire $y$ domain of the fully nonlinear equation Eq. (6). Figure 2 shows the different types of shock wave propagating in a sonic vacuum for different values of $\bar{p}$ by solving Eq. (6) using Matlab. The critical value $\bar{p}_{c,\mathrm{sv}}=1.265$ was obtained from Eq. (18) using $y_2=1$ and $n=3/2$ corresponding to a Hertzian interaction.

The value of $y=0$ at point $\eta=0$ corresponds to the $y_1$, the local maximum of $W(y)$ for curve (1) in Fig. 1. In the numerical solution to Eq. (6), in the strongly nonlinear regime, an initial displacement of $\Delta y=0.001$ was given to $y$ to start motion from the point corresponding to $y_1=0$ ($\Delta y$ is equal to 0.1% of the final $y_2$ value). The shock profile corresponding to the critical viscosity $\bar{p}=\bar{p}_{c,\mathrm{sv}}$ is shown in curve (1) in Fig. 2. It is apparent that the value of $\bar{p}_{c,\mathrm{sv}}$ adequately describes the transition from the oscillatory to monotonic profile shown in curves (4)–(1) in Fig. 2.

We conclude that even though the expression for $\bar{p}_{c,\mathrm{sv}}$ is derived in the vicinity of the final state of the shock wave, it represents the global transition from oscillatory to monotonic shock profiles in the strongly nonlinear regime corresponding to a sonic vacuum.

Remarkably, the reduction of the viscosity resulting in the transition from a monotonic to an oscillatory shock front does not dramatically reduce the shock onset width (Fig. 2). The term shock onset width is used here to describe the distance, in $\eta$, from the initial state to the maximum of the first peak of the shock front. This can be partially explained because the shock onset width is limited by the half-width of the solitary wave solution in a nondissipative system as $\bar{p}\to 0$. The equation for the width of a strongly nonlinear solitary wave in a sonic vacuum for particles interacting according to a general power law is [1]

$$L_s=\pi a/(n-1)\sqrt{n(n+1)/6}, \tag{20}$$

where $a$ is the particle diameter. The width of a strongly nonlinear solitary wave can be expressed in terms of $\eta$ for comparison with the shock onset width seen in Fig. 2. Dividing this expression by two gives the nondimensional limit of shock onset-width corresponding to a very low viscosity,

$$\bar{L}_s/2=\pi(n+1)/(2n-2). \tag{21}$$

Substituting $n=3/2$ into this expression results in an onset width of 7.8, which is very close to the width shown in curve (4) in Fig. 2 for a relatively small dissipation value $\bar{p}=0.25\bar{p}_{c,\mathrm{sv}}$.

It is important to note that the width of the shock front is the distance from the initial state, $y_1$, to the steady final state, $y_2$, which is significantly larger than the onset width for the oscillatory shock profile. The width of the monotonic shock wave corresponding to $\bar{p}_{c,\mathrm{sv}}$ is approximately $7a$, which is about 3 times greater than the solitary wave half-width in a nondissipative strongly nonlinear sonic vacuum type system [see curve (1) in Fig. 2]. In an overdamped system, where $\bar{p}>\bar{p}_{c,\mathrm{sv}}$, the width of the shock front and onset-width are identical and increase with increasing viscosity. For an underdamped system, where $\bar{p}<\bar{p}_{c,\mathrm{sv}}$, the shock front width is again longer than in the critically damped case due to the oscillatory tail. For example, compare curve (4) in Fig. 2, where $\bar{p}=0.25\bar{p}_{c,\mathrm{sv}}$ to curve (1) in Fig. 2, $\bar{p}=\bar{p}_{c,\mathrm{sv}}$.

It is interesting that a long shock front width that is significantly larger than distance between particle centers exists in two distinct cases corresponding to qualitatively different paths to the final state. In the case of weak dissipation the final state is attained through multiple, slightly damped, oscillations. In the case of a relatively strong dissipation, where $p>p_c$, the final state is attained very slowly without oscillations. As a result the shock front width is minimal in a critically damped system at $p=p_c$.

The critical viscosity given by Eq. (17) corresponds to the transition from an oscillatory to a monotonic shock profile in the general case including both strongly and weakly nonlinear regimes. It is interesting to compare this prediction of the critical viscosity in a weakly nonlinear case with the behavior of solution of Eq. (6). Oscillatory and monotonic profiles of $y$ corresponding to Eq. (6) in the weakly nonlinear potential $W(y)$ (for values of $C_3$ close to 5/27) were obtained using Matlab and are shown in Fig. 3. In the numerical solution of Eq. (6), a value of $C_3=49999/270000$ was used, which is slightly smaller than critical value $C_3=5/27$. For this value of $C_3$, the initial and final state in the shock wave are $y_1=0.3605474$ and $y_2=0.3652323$. An initial displacement of 0.1% of the difference between the starting and final $y$ values ($\Delta y=4.7\times 10^{-6}$) was given to $y$ to start a motion from $y_1$.

In a strongly precompressed system the behavior of the solution in the vicinity of $y_2$ is expected to closely match the global behavior of the solution because the change of strain

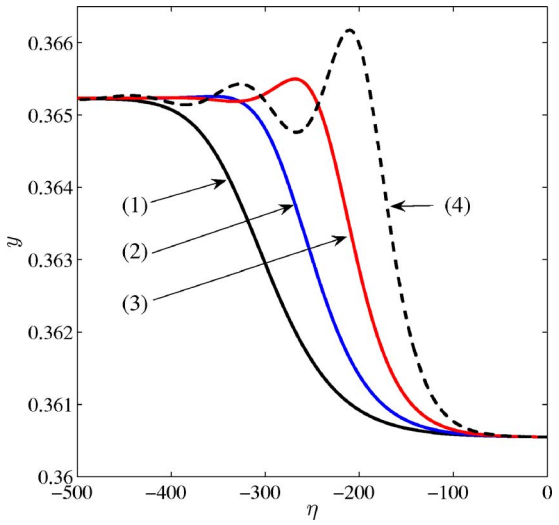


FIG. 3. (Color online) Oscillatory and monotonic shock waves in a weakly nonlinear lattice ($C_3$=49999/270000). In this plot of the numerical solution of Eq. (6) the calculated $\bar{p}_{c,w}$ value is 0.074 and curves (1)–(4) in the figure show the solution at different values of $\bar{p}$. Curve (1) corresponds to $\bar{p}=\bar{p}_{c,w}$, curve (2) to $\bar{p}=0.75\bar{p}_{c,w}$, curve (3) to $\bar{p}=0.5\bar{p}_{c,w}$, and curve (4) to $\bar{p}=0.25\bar{p}_{c,w}$.

in the wave is small compared to the initial strain in the system. The decrease of viscosity from the critical value $\bar{p}_{c,w}$ [calculated using Eq. (17)] to the smaller values $0.75\bar{p}_{c,w}$, $0.5\bar{p}_{c,w}$ and $0.25\bar{p}_{c,w}$ corresponds to the transition from the monotonic profile shown in curve (1) in Fig. 3 to the oscillatory shock profiles in curves (2), (3), and (4).

The equation for the critical viscosity in a dissipative system that behaves according to the weakly nonlinear KdV equation [which is a partial case of Eq. (3)] is derived in [18]. We can relate the general equation for the critical viscosity Eq. (17) with the known result of the partial weakly nonlinear case using $n=3/2$ for the Hertzian potential between particles for future comparison with experiments. Also, the KdV equation with dissipation can be easily obtained from Eq. (3) to apply results of [18] directly.

It is assumed that the weakly nonlinear system is initially compressed resulting in initial strain $\xi_0$ and that any traveling wave is a small perturbation: $\xi=\xi_0+\varepsilon$, where $\varepsilon/\xi_0 \ll 1$. This ratio is the second small parameter we need to derive the weakly nonlinear equation in addition to $R/L \ll 1$ required for the long wave approximation, where $L$ is the characteristic wavelength. The resulting wave equation takes the form of the KdV equation including dissipation when written for a wave traveling in one direction,

$$\varepsilon_t - \hat{p}_w \varepsilon_{xx} + c_0 \varepsilon_x + \left(\gamma - \frac{\hat{p}_w^2}{2c_0}\right)\varepsilon_{xxx} + \frac{\sigma}{2c_0}\varepsilon\varepsilon_x = 0, \quad (22)$$

where $\hat{p}_w \equiv 2R^2 p$ is the viscosity coefficient for a system that permits weakly nonlinear waves (thus the subscript $w$) and has units of dynamic viscosity and

$$\delta_0 = 2R\xi_0, \quad c_0^2 = 6AR^2\delta_0^{1/2}, \quad \sigma = c_0^2 R/\delta_0,$$

$$c^2 = A(2R)^{5/2}, \quad \gamma = c_0 R^2/6. \quad (23)$$

Note that Eq. (22) contains a second order correction to the dissipative term. We can neglect this term because $p_c \to 0$ as $y_2$ and $C_3$ approach their critical values [see curves (4) and (5) in Fig. 1]. The equation for critical viscosity for this weakly nonlinear system based on [18] is

$$p_{c,w} = \frac{c_0}{\sqrt{6}R}\sqrt{\frac{V_{\rm sh}}{c_0} - 1}. \quad (24)$$

Equation (24) can also be obtained as the limit of the critical viscosity in the general strongly nonlinear case given by Eq. (17) as $V_{\rm sh} \to c_0$. For a Hertzian interaction, $n=3/2$ is placed into Eq. (17) along with the definition of $\bar{p}$ from Eq. (7),

$$p_c = \frac{V_{\rm sh}}{2\sqrt{2}R}\sqrt{\frac{3}{2}y_2^{4/5} - y_2^{2/5}}. \quad (25)$$

To write this equation in terms of the speed of the shock wave $V_{\rm sh}$ and initial sound speed $c_0$ we can use the relation between $y_2$ and $y_1$ [27]

$$y_2 = \left[\frac{1}{2}\left(1 - y_1^{2/5} + \sqrt{(1-y_1^{2/5})(1+3y_1^{2/5})}\right)\right]^{5/2}. \quad (26)$$

Using the expressions for $c_0$,

$$c_0^2 = 3/2\,\xi_0^{1/2}c^2, \quad (27)$$

and for $y_1$ in terms of $c_0$ and $V_{\rm sh}$,

$$y_1 = (2/3)^{5/2}\left(\frac{c_0}{V_{\rm sh}}\right)^5, \quad (28)$$

and substituting Eqs. (26)–(28) into Eq. (25) obtain

$$p_c = \frac{c_0}{4\sqrt{2}R}\left[\frac{4}{3} - \frac{4}{3}\left(\frac{c_0}{V_{\rm sh}}\right)^2 + \left(\frac{c_0}{V_{\rm sh}}\right)^{-2} + \left(1 - 2\left(\frac{c_0}{V_{\rm sh}}\right)^2\right)\sqrt{\left(\frac{c_0}{V_{\rm sh}}\right)^{-4} + \frac{4}{3}\left(\frac{c_0}{V_{\rm sh}}\right)^{-2} - \frac{4}{3}}\right]^{1/2}. \quad (29)$$

For a weakly nonlinear system, $V_{\rm sh}=c_0+\Delta(\Delta/c_0 \ll 1)$, and this small parameter can be used to expand Eq. (29). This expansion results in the critical viscosity in the weakly nonlinear system,

$$p_{c,w} = \sqrt{\frac{c_0\Delta}{6R^2}}. \quad (30)$$

Equation (24) is recovered from Eq. (30) with the replacement $\Delta=V_{\rm sh}-c_0$. Thus Eq. (17) describing the transition from oscillatory to monotonic shock profiles in a general strongly nonlinear case is consistent with the known equation for the critical viscosity in a weakly nonlinear system.

## IV. NUMERICAL INVESTIGATION OF THE CRITICAL VISCOSITY IN A DISCRETE SYSTEM

The numerical analyses of a discrete particle lattice are presented here for comparison with the results based on the

long-wave approximation leading to the value of critical viscosity, Eq. (17). There are differences between applied analytical approach in the frame of the long wave approximation and the numerical calculations of discrete particle lattice. First, the analytical approach assumes a stationary profile with a constant shock wave speed but does not account for the transient development of the wave into its steady state. Also, it is important to compare the critical viscosity value derived from the long wave approximation to a value characteristic for shock waves in discrete chains because the width of a weakly dissipative shock is comparable to the size of the particles; especially for large values of $n$. These features may result in significantly disparate behaviors of the shock wave solutions of the long wave approximation and the discrete lattice.

The numerical analyses will test how well Eqs. (17) and (18) predict the transition from an oscillatory to a monotonic shock profile in a discrete system even though the expressions for $p_c$ rely on the behavior of solution in the vicinity of the final state of the shock wave. This numerical investigation will focus on a sonic vacuum type system since the solution based on the long wave approximation is expected to be a better fit to the behavior of a discrete system in the weakly nonlinear regime.

A shock wave is created in the numerical simulation by prescribing a constant velocity $v_0$ to the first particle of an initially quiescent lattice at $t=0$. The discrete displacement solution is used to find the strains for comparison with the long-wave approximation. The equation for the strain $\xi$ in a discrete lattice taken between particles $i$ and $i+1$ is defined as

$$\xi = (u_i - u_{i+1})/2R. \tag{31}$$

To compare numerical results for developing and stationary shock waves in a discrete lattice with the stationary solution in the long wave approximation the particle velocity in the final state in the shock wave is assumed to be equal to the velocity of the first particle in the numerical calculations. It should be mentioned that final state of the shock wave in a sonic vacuum in the long wave approximation corresponds to the value of $y=1$ (see Fig. 1) resulting in the following relations between shock speed $V_{\mathrm{sh}}$, particle velocity $v_0$ and strain $\xi_{\mathrm{sh}}$ in the final state:

$$V_{\mathrm{sh}} = c_n^{2/(n+1)} v_0^{(n-1)/(n+1)} = c_n \xi_{\mathrm{sh}}^{(n-1)/2}. \tag{32}$$

The plots of the numerical calculations and the curves obtained in the long wave approximation are presented in nondimensional coordinates $y$ and $\eta$:

$$y = (c_n/v_0)\xi^{(n+1)/2}, \tag{33}$$

$$\eta = -\frac{c_n^{2/(n+1)} v_0^{(n-1)/(n+1)} t}{2R} \sqrt{6(n+1)/n}. \tag{34}$$

Equations (31)–(34) are used to plot the numerical data in Figs. 4–6.

We compare the numerical solution for oscillatory and monotonic shock waves in a discrete lattice with the long wave approximation in case when $n=3/2$ for spheres interacting with a Hertzian potential. The data in Table I were selected to resemble a real system similar to those found in previous experimental work [6,17,28] for the purpose of future comparison with experiments. The expression for $A$ in

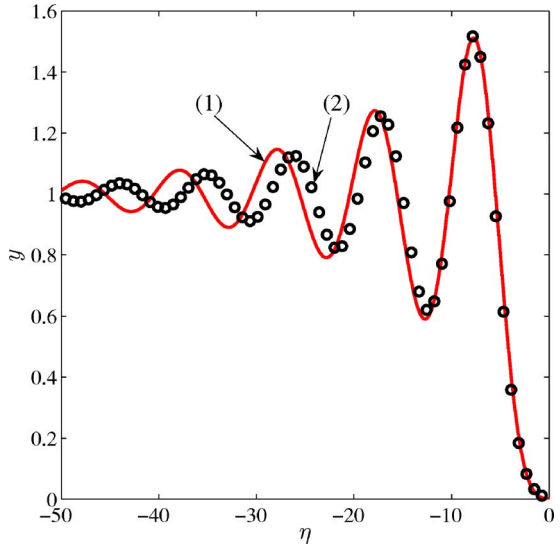


FIG. 4. (Color online) An oscillatory shock wave in a strongly nonlinear lattice close to the impacted end. Curve (1): The numerical solution of the long-wave approximation, Eq. (6), for $\bar{p}=0.1\bar{p}_{c,\mathrm{sv}}$. Curve (2): The circles represent the path of $y$ in a discrete particle lattice for the interaction of the 15th and 16th particle from $t=48.13$ $\mu$s (far right) to $t=102.4$ $\mu$s from the beginning of impact (far left) with the same value of viscosity. For convenience, both curves are plotted from the moment of arrival of the shock wave at a given point.

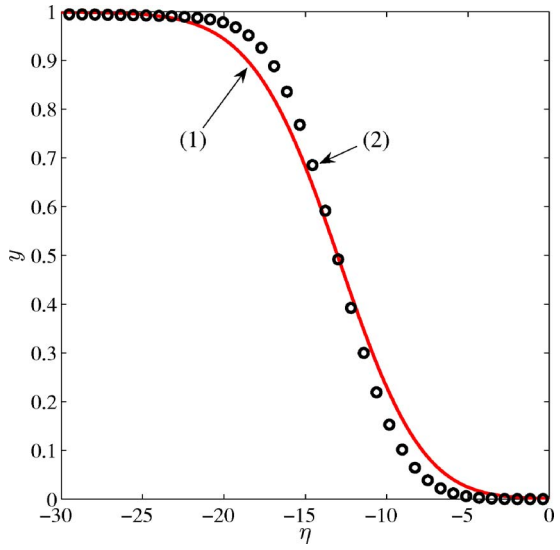


FIG. 5. (Color online) Comparison of the early development of a monotonic shock wave in a discrete strongly nonlinear lattice and stationary solution in the long wave approximation. Curve (1): The solid line is a plot of the solution of the long-wave approximation, $y(\eta)$, for $\bar{p}=\bar{p}_{c,\mathrm{sv}}$. Curve (2): The circles represent the path of $y$ in a discrete lattice for the interaction of the fifth and sixth particle from $t=5$ $\mu$s to $t=35$ $\mu$s. For convenience both curves are plotted from the moment of arrival of the shock wave at a given point.

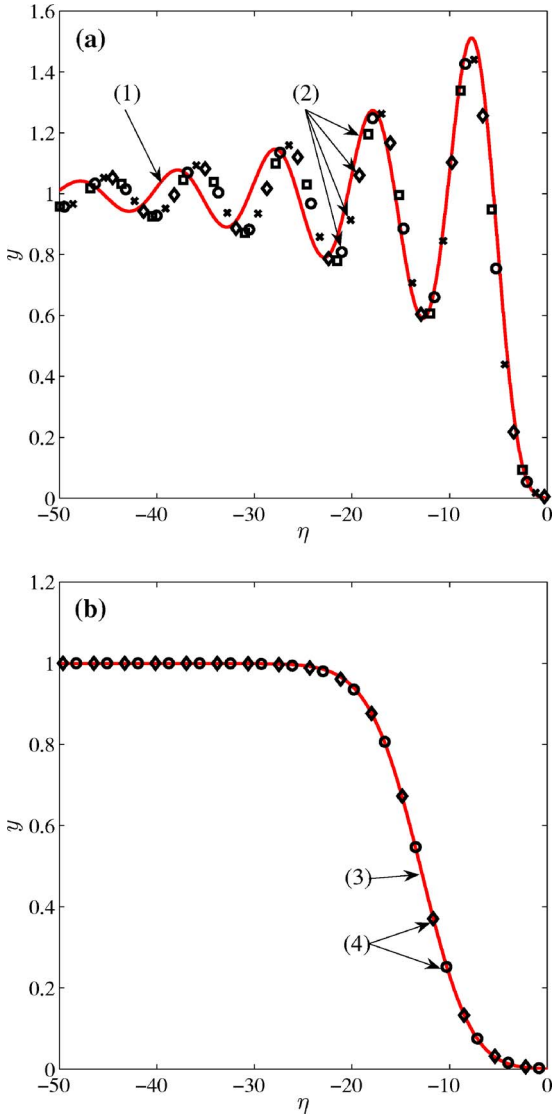


FIG. 6. (Color online) Comparison of (a) oscillatory and (b) monotonic steady shock waves in a discrete strongly nonlinear lattice and the results of the long wave approximation. Curve (1) is the stationary solution of the long wave approximation for an oscillatory shock front; curve (2) is a set of discrete points representing the parameter $y$ related to the strain between particles: □—particle contacts 218–234 at time $t \cong 1638$ $\mu$s; ◇—particle contacts 454–468 at $t \cong 3278$ $\mu$s; ×—particle contacts 685–701 at $t \cong 4918$ $\mu$s; ○—particle contacts 919–934 at $t \cong 6557$ $\mu$s; curve (3) is a stationary solution of the long wave approximation for a monotonic shock front; curve (4) is a set of discrete points representing the parameter $y$ between particles for comparison with curve (3): ◇—particle contacts 455–470 at $t \cong 3278$ $\mu$s; ○—particle contacts 921–937 at $t \cong 6557$ $\mu$s. For convenience all curves are plotted from the moment of arrival of the shock wave at a given point.

Eq. (2) assumes a homogeneous particle mass and radius throughout the lattice: $A = E(2R)^{1/2}/[3m(1-\nu^2)]$, where $m = 4/3\pi R^3 \rho_0$. The values of $p$ in the numerical simulation of a discrete lattice were $p = 0.1p_{c,\mathrm{sv}}$ and $p = p_{c,\mathrm{sv}}$; the values of $p_{c,\mathrm{sv}}$ were calculated from the combination of Eq. (19) and Eq. (32) and the parameters from Table I.

TABLE I. Parameters used in numerical analysis.

| | Symbol | Units | Value |
|---|---|---|---|
| Young's modulus | $E$ | (GPa) | 193 |
| Poisson's ratio | $\nu$ | | 0.3 |
| Density | $\rho$ | (kg/m$^3$) | 8000 |
| Particle radius | $R$ | (m) | $2.38 \times 10^{-3}$ |
| Mass | $m$ | (kg) | $4.52 \times 10^{-4}$ |
| Critical viscosity | $\mu_{\mathrm{cr}}$[a] | (Ns/m) | 32.15 |
| Number of particles | $N$ | | 1000 |
| Initial velocity | $v_0$ | (m/s) | 0.5 |
| Time step | $\delta t$ | ($\mu$s) | 0.875 |

[a] $\mu_{\mathrm{cr}} = mp_c$.

Figure 4 depicts the early development of an oscillatory shock wave in a discrete lattice in comparison with the results of long wave approximation using $p = 0.1p_{c,\mathrm{sv}}$. Time $t$ is calculated starting from the moment of arrival of shock wave at given point of observation. The points comprising curve (2) in Fig. 4 are the discrete $y$ values between the 15th and 16th particles. Note the progressive phase shift between oscillations, slightly larger amplitude of the first peak, and the smaller amplitudes of the oscillations behind it in comparison to the analytical solution shown in curve (1). Despite these differences, the qualitative behavior of the oscillatory shock wave matches well with the long-wave approximation in this unsteady regime of propagation close to the impacted end of the lattice.

The early development of a monotonic shock profile at a distance close to the impacted end in a discrete lattice is shown in curve (2) in Fig. 5 for the critical viscosity $p_{c,\mathrm{sv}}$ derived from the long wave approximation. Curve (1) in Fig. 5 represents the stationary profile of a shock wave in the long wave approximation [it is identical to curve (1) in Fig. 2] for comparison to the results for discrete lattice. The $y$ values for the contact between fifth and sixth particles are shown from times $t = 5$ $\mu$s to $t = 35$ $\mu$s starting from the moment of impact.

In this unsteady state of shock propagation, curve (2) in Fig. 5 oscillates slightly as it approaches $y = 1$ behind the shock front and the shock onset width is less than that of curve (1). It is interesting that, despite this tiny oscillation, the qualitative shape of the shock profile closely resembles the steady state solution for the long-wave approximation. This shows that the critically damped shock profile in a strongly nonlinear discrete system approaches a stationary state after traveling only a few particles after formation.

In Figs. 4 and 5 the unsteady shock profiles formed near the impacted end were compared to the stationary solution in long-wave approximation. It is interesting to compare them at larger distances from the impacted end where shock profiles in the discrete lattice should be closer to a shape corresponding to steady state of shock propagation.

The corresponding data for both oscillatory and monotonic profiles in the long wave approximation and in the discrete lattice at a few distances from entrance are shown in Fig. 6. Curve (1) in Fig. 6(a) is identical to curve (1) in Fig.

4. Curve (4) in Fig. 6(b) closely matches the long-wave approximation curve (3) for the monotonic shock wave. We assume that if a profile is not changing qualitatively after traveling through a few hundred particle contacts, it is steady enough for the present discussion.

The difference in shock-front widths in curve (2) (Fig. 5) is indistinguishable when compared to curve (2) in Fig. 6(b). This means that the critical value of viscosity $p_{c,\mathrm{sv}}$ from Eq. (19) captures the transition from oscillatory to monotonic wave profiles in discrete lattice very well on the stationary stages of shock wave propagation.

## V. CONCLUSIONS

The long-wave approximation of a strongly nonlinear system with a power law dependence of force on displacement was extended to include viscous dissipation that depends on the relative velocities of neighboring particles. From this approach an equation for a critical viscosity describing the transition from oscillatory to monotonic shock profiles in a strongly nonlinear regime was derived. This equation naturally includes the weakly nonlinear case. Numerical calculations of the discrete system agreed well with the results of long wave approximation. It should be emphasized that the initial disturbance in a discrete chain approaches a stationary shock regime at a distance comparable to the width of the stationary shock front from the boundary particle. This is analogous to the case of a nondissipative system where the initial disturbance forms a single or a train of solitary waves after traveling a short distance that is comparable to the width of the leading pulse of a stationary shock front. The shock onset width was defined and compared with the width of a solitary wave. The shock front width is minimized when the viscosity is equal to its critical value.

## ACKNOWLEDGMENTS

The authors wish to acknowledge the support of this work by the U.S. NSF (Grant No. DCMS03013220).

[1] V. F. Nesterenko, *Dynamics of Heterogeneous Materials* (Springer-Verlag, New York, 2001).
[2] V. F. Nesterenko, Fiz. Goreniya Vzryva **28**, 121 (1992).
[3] V. F. Nesterenko, in *Proceedings of Second International Symposium on Intense Dynamic Loading and Its Effects* (Chengdu, China, 1992), pp. 236–240.
[4] V. F. Nesterenko, in *Akustika neodnorodnykh sred* (Nauka, Novosibirsk, 1992), pp. 228–233.
[5] V. F. Nesterenko, *High-Rate Deformation of Heterogeneous Materials* (Nauka, Novosibirsk, 1992).
[6] C. Daraio, V. F. Nesterenko, E. B. Herbold, and S. Jin, Phys. Rev. E **73**, 026610 (2006).
[7] C. Daraio, V. F. Nesterenko, E. B. Herbold, and S. Jin, Phys. Rev. E **72**, 016603 (2005).
[8] A. Rosas, D. ben-Avraham, and K. Lindenberg, Phys. Rev. E **71**, 032301 (2005).
[9] P. Gondret, M. Lance, and L. Petit, Phys. Fluids **14**, 643 (2001).
[10] A. Stocchino and M. Guala, Exp. Fluids **38**, 476 (2005).
[11] R. Ramìrez, T. Pöschel, N. V. Brilliantov, and T. Schwager, Phys. Rev. E **60**, 4465 (1999).
[12] N. V. Brilliantov, F. Spahn, J.-M. Hertzsch, and T. Pöschel, Phys. Rev. E **53**, 5382 (1995).
[13] A. Rosas and K. Lindenberg, Phys. Rev. E **68**, 041304 (2003).
[14] M. Manciu, S. Sen, and A. J. Hurd, Physica D **157**, 226 (2001).
[15] G. E. Duvall, R. Manvi, and S. C. Lowell, J. Appl. Phys. **40**, 3771 (1969).
[16] C. Brunhuber, F. G. Mertens, and Y. Gaididei, Phys. Rev. E **73**, 016614 (2006).
[17] E. B. Herbold, V. F. Nesterenko, and C. Daraio, in *Proceedings of the Conference of the American Physical Society Topical Group on Shock Compression of Condensed Matter*, AIP Conf. Proc. No. 845 (AIP, Melville, NY, 2006), pp. 1523–1526; e-print cond-mat/0512367.
[18] V. Karpman, *Nonlinear Waves in Dispersive Media* (Pergamon Press, New York 1975).
[19] G. Friesecke and J. A. D. Wattis, Commun. Math. Phys. **161**, 391 (1994).
[20] V. F. Nesterenko, Prikl. Mekh. Tekh. Fiz. **5**, 136 (1983), [J. Appl. Mech. Tech. Phys. **5**, 733 (1984)].
[21] E. Hascoët and H. Herrmann, Eur. Phys. J. B **14**, 183 (2000).
[22] A. Rosas and K. Lindenberg, Phys. Rev. E **69**, 037601 (2004).
[23] I. A. Kunin, *Theory of Elastic Media with Microstructure* (Nauka, Moscow, 1975) (in Russian).
[24] A. Chatterjee, Phys. Rev. E **59**, 5912 (1999).
[25] E. Hinch and S. Saint-Jean, Proc. R. Soc. London, Ser. A **455**, 3201 (1999).
[26] C. Arancibia-Bulnes and J. Ruiz-Suàrez, Physica D **168-169**, 159 (2002).
[27] C. Coste, E. Falcon, and S. Fauve, Phys. Rev. E **56**, 6104 (1997).
[28] V. F. Nesterenko, C. Daraio, E. B. Herbold, and S. Jin, Phys. Rev. Lett. **95**, 158702 (2005).